· Review · Advances in Polar Science
doi: 10.13679/j.advps.2021.0026 December 2021 Vol. 32 No. 4: 295-311

An overview of Antarctic polynyas: sea ice production, forcing mechanisms, temporal variability and water mass formation

WEI Zheng[1], ZHANG Zhaoru[1*], Timo VIHMA[2], WANG Xiaoqiao[1] & CHEN Yuanjie[1]

[1] School of Oceanography, Shanghai Jiao Tong University, Shanghai 200240, China;
[2] Meteorological Research, Finnish Meteorological Institute, FI-00560 Helsinki, Finland

Received 21 June 2021; accepted 10 September 2021; published online 15 November 2021

Abstract Polynyas are irregular open water bodies within the sea ice cover in polar regions under freezing weather conditions. In this study, we reviewed the progress of research work on dynamical forcing, sea ice production (SIP), and water mass formation for both coastal polynyas and open-ocean polynyas in the Southern Ocean, as well as the variability and controlling mechanisms of polynya processes on different time scales. Polynyas play an irreplaceable role in the regulation of global ocean circulation and biological processes in regional ocean ecosystems. The coastal polynyas (latent heat polynyas) are mainly located in the Weddell Sea, the Ross Sea and on the west side of protruding topographic features in East Antarctica. During the formation of coastal polynyas, which are mainly forced by offshore winds or ocean currents, brine rejection triggered by high SIP results in the formation of high salinity shelf water, which is the predecessor of the Antarctic bottom water — the lower limb of the global thermohaline circulation. The open-ocean polynyas (sensible heat polynyas) are mainly found in the Indian sector of the Southern Ocean, which are formed by ocean convection processes generated by topography and negative wind stress curl. The convection processes bring nutrients into the upper ocean, which supports biological production and makes the polynya regions an important sink for atmospheric carbon dioxide. The limitations and challenges in polynya research are also discussed.

Keywords **Antarctic polynyas**, **forcing mechanisms, sea ice production**, **water mass formation**, **temporal variability**

Citation: Wei Z, Zhang Z R, Vihma T, et al. An overview of Antarctic polynyas: sea ice production, forcing mechanisms, temporal variability and water mass formation. Adv Polar Sci, 2021, 32(4): 295-311, doi: 10.13679/j.advps.2021.0026

1 Introduction

Polynyas are irregular open sea water bodies (10 km^2 to 2–3×10^5 km^2) surrounded by sea ice or regions of significantly reduced sea ice cover during atmospheric freezing conditions (Smith et al., 1990; Barber et al., 2001; Morales Maqueda, 2004). In the Southern Ocean, the size of major polynyas varies from region to region, which ranges from a few hundred meters to hundreds of kilometers (Smith et al., 1990), and polynyas occur recurrently in fixed regions (Morales Maqueda, 2004). Polynyas usually occur in austral autumn and winter, and can have strong interannual variations in the duration time (Geddes and Moore, 2007; Qian et al., 2020).

By the formation and maintenance mechanisms, polynyas in the Southern Ocean can be categorized into two classic types: sensible heat polynyas and latent heat polynyas. Sensible heat polynyas are also known as "open-ocean polynyas", which are large openings in the

* Corresponding author, ORCID: 0000-0001-6125-8660, E-mail: zrzhang@sjtu.edu.cn

winter sea ice cover and maintained by the upwelled heat through convective mixing (Campbell et al., 2019). The upwelled heat melts pre-existing sea ice and prevents the growth of new ice. Since the start of modern satellite passive microwave observations in the 1970s, two prominent open-ocean polynyas have been observed in the Southern Ocean. The larger one occurs intermittently in the Weddell Sea near the Maud Rise seamount (Cheon and Gordon, 2019), while the smaller one occurs recurrently in the Cosmonaut Sea along the far eastern margin of the Weddell gyre and the open-ocean off the Enderby Land (Comiso and Gordon, 1987, 1996). The latent heat polynyas are formed and maintained by the divergence of sea ice due to coastal winds typically dominated by katabatic winds (Comiso and Gordon, 1996; Tamura et al., 2008) or oceanic currents (Arbetter, 2004; Morales Maqueda, 2004). Coastal sea ice is blown off the shore, which causes high sea ice production (SIP) in Antarctic coastal polynyas (Nihashi and Ohshima, 2015). The extent of latent heat polynyas is the result of balance between the export of sea ice from polynyas and the SIP within the polynyas (Morales Maqueda, 2004). Applying the Polynya Signature Simulation Method (PSSM), Kern (2009) analyzed the satellite observations and found that the coastal polynyas along East Antarctica contributed about 40% of the total polynya area of the Southern Ocean, and the coastal polynyas in the Weddell Sea and Ross Sea together contributed 30%.

Polynyas host many important physical and biological oceanic processes. The brine rejection process during the formation of latent heat polynyas and ocean-atmosphere heat exchange lead to the densification of surface water, which accelerates the formation of High Salinity Shelf Water (HSSW) (Kusahara et al., 2011b). HSSW mixes with the Circumpolar Deep Water (CDW) intruding onto the continental shelves and ice shelf meltwater, and sinks across the continental slope, leading to the formation of Antarctic Bottom Water (AABW) that contributes to the lower limb of the global meridional overturning circulation (Stössel et al., 2002; Jacobs, 2004; Marshall and Speer, 2012; Tamura et al., 2016). The formation of HSSW and AABW has been studied in many coastal regions, such as the Weddell Sea (Naveira Garabato et al., 2002), the Ross Sea (Whitworth and Orsi, 2006), the Prydz Bay (Yabuki et al., 2006; Williams et al., 2016), the Cape Darnley Polynya (Ohshima et al., 2013), the Vincennes Bay Polynya (Kitade et al., 2014), and the Mertz Polynya (Williams et al., 2010; Ohshima et al., 2016). In addition to coastal regions, AABW may have been formed predominantly in open-ocean polynyas in past glacial periods. Govin et al. (2009) established a glacial ocean circulation and found that the sea ice formation during winters and the deep convection of poorly ventilated AABW were enhanced in the Southern Ocean during the last glacial inception, which might be associated with the open-ocean polynyas. Wang et al. (2017) found that the deep convection that occurred in the Weddell Polynya (WP) in a high-resolution ocean-sea-ice model would cool the deep layer and the cooled water would be transported towards the shelf regions by meanders and eddies. Meanwhile, the cooled water would be transported westward by an intensified slope current. Polynyas also play a significant role in regional ecosystems and are known as “oases” of the Southern Ocean. The Southern Ocean ecosystem is characterized by high-nutrient but low-chlorophyll because of the iron limitation (Blain et al., 2007). Upwelling in polynya areas can bring iron from deep water to the surface layer of the ocean, which sustains higher primary production when polynyas are exposed to atmosphere and receive solar radiation earlier than surrounding regions (Mundy and Barber, 2001; Arrigo, 2003; Planquette et al., 2013; Klunder et al., 2014). The primary production of polynyas serves as the base of the food chains and the polynyas also provide habitats for high-trophic-level species, such as sea birds (Gilchrist and Robertson, 2000), seals (McMahon et al., 2004), etc. It is found that upwelling in the Maud Rise Polynya (MRP) provided sufficient nutrients in austral spring and caused the occurrence of phytoplankton blooms (Jena and Pillai, 2020). High primary production and the existence of deep convection also make polynyas crucial carbon dioxide reservoirs in the Southern Ocean and an important part of carbon cycling system (Arrigo et al., 1998; Hoppema and Anderson, 2007; Miller and DiTullio, 2007).

Polynyas also play a significant role in modulating Antarctic atmospheric processes. Due to high SIP in coastal polynyas, the heat loss is one or two orders of magnitude larger than that in areas covered by thick ice (Maykut, 1978) and reaches several hundred Watts per square meter (Willmott et al., 2007). For example, the heat loss in the Terra Nova Bay Polynya (TNBP) reached its maximum in the 2003 (313 $W \cdot m^{-2}$). Therefore, the heat and moisture released by the formation of coastal polynyas have significant effects on the mesoscale atmospheric motions over the polynya regions (Alam and Curry, 1995; Gallée, 1997). It has been proved by numerical simulations that open-ocean polynyas in the Southern Ocean have local impacts on turbulent heat fluxes, precipitation, cloud characteristics and radiative fluxes. Weijer et al. (2017) analyzed the simulations from a Community Earth System Model resolving atmospheric and oceanic synoptic-scale processes and found that the sensible and the latent heat fluxes were enhanced over the open-ocean polynya and could reach 125 and 84 $W \cdot m^{-2}$ in August, which were typically 110 and 72 $W \cdot m^{-2}$ higher than those during non-polynya years.

This review work is organized as follows. In Section 2, the driving forces of coastal polynyas are introduced, followed by the descriptions of the SIP characteristics and temporal variations of sea ice and oceanic processes on different time scales. In Section 3, the forcing mechanisms of open-ocean polynyas are first introduced. The linkage between the behaviors of open-ocean polynyas with

large-scale climate modes, such as the Southern Annular Mode (SAM) and the El Niño-Southern Oscillation (ENSO) are presented. In Section 4, the limitations and challenges of current research on Antarctic polynya processes are discussed.

2 Antarctic coastal polynyas

2.1 The driving force of coastal polynyas

2.1.1 Boundary conditions

Typically occurring over shallow continental shelves (Zwally et al., 1985), Antarctic coastal polynyas are so-called latent-heat polynyas. It means that the polynya water is approximately at the freezing point, and there is a balance between frazil ice formation in the polynya and ice export out of the polynya (Gordon and Comiso, 1988; Morales Maqueda, 2004). The frazil ice formation results in loss of latent heat from the ocean to the atmosphere. The ice transport is mainly caused by offshore wind forcing, particularly the katabatic wind (Kwok et al., 2007; Nihashi and Ohshima, 2015), while tidal or ocean currents may also contribute (Morales Maqueda, 2004).

In addition to atmospheric and oceanic forcing, geographic factors are important in controlling where and when coastal polynyas form in the Antarctic. The factors include orography of land and ice sheet, geometry of the coastline, topography of the ocean floor, and obstacles, such as grounded ice bergs and glacier tongues (Nøst and Østerhus, 1985; Gordon and Comiso, 1988; Morales Maqueda, 2004; Lacarra et al., 2014; Tamura et al., 2016). Polynyas occur most commonly when the obstacles are oriented in the north-south direction, preventing sea ice transport by easterly winds, which dominate over the Antarctic coastal zone (Massom et al., 1998). Recurrent coastal polynyas typically form in locations where the above-mentioned factors are favorable and offshore winds or currents prevail (Kurtz and Bromwich, 1985; Kusahara et al., 2011a). Occasional formation of polynyas can take place in any location where the atmospheric or oceanic dynamical forcing is strong enough to push the ice away from the coast and there is no obstacle preventing the ice transport. The forcing and boundary conditions control the polynya size. During winter, the width of an Antarctic coastal polynya is typically a few kilometers and practically always less than 50 km (Markus and Burns, 1995). In spring and summer, when sea ice melts and solar heating of the sea increases, the coastal polynyas typically grow (Morales Maqueda, 2004) until they are merged with the open ocean.

Due to the typically dominating effect of wind forcing on ice drift, the occurrence and size of coastal polynyas vary a lot in time (Renfrew, 2002), mostly at the daily scale, followed by monthly and seasonal scales (Ward, 2018). The boundary conditions related to orography/icescape typically vary slowly, but also abrupt changes may occur, e.g. due to ice shelf collapse or grounding of an iceberg, which may rapidly change the polynya occurrence or size (Nøst and Østerhus, 1985). On the decadal time scale, the cumulative area of the 25 Antarctic coastal polynyas studied by Ward (2018) had a statistically significant positive trend from 1992 to 2017.

2.1.2 Local wind over polynyas

The local near-surface wind is the most direct atmospheric factor causing opening of coastal polynyas, keeping them open, and controlling their size. Lebedev (1968) presented an analytic model for the balance of a coastal polynya between the wind-driven ice drift divergence and heat loss from the sea surface via turbulent and radiative fluxes. Pease (1987) further developed the model, and found that under a certain offshore wind velocity, colder air results in a smaller polynya. If the wind speed increases, the polynya becomes wider, but the effect is not dramatic. This is because an increasing wind speed simultaneously increases the ice drift speed, favoring a wider polynya and more turbulent fluxes from the polynya to the atmosphere, resulting in more ice production and hence a narrower polynya.

The formation of coastal polynyas is controlled by the local wind, which is typically generated via katabatic or synoptic forcing. The speed of the katabatic wind depends on the slope height and steepness as well as on the efficiency of radiative cooling that generates the stable stratification over the ice sheet and thus the gravitational forcing for the airflow (Gallée, 1997; Vihma et al., 2011). A flat ice shelf between the slope and the ocean strongly decelerates the near-surface katabatic wind, and its core may rise over the cold air pool often generated on an ice shelf (Vihma et al., 2011). Depending on the coastline and icescape geometry, either offshore katabatic winds or prevailing easterly winds may be important for the formation of coastal polynyas (Massom et al., 1998). According to Adolphs and Wendler (1995) and Wendler et al. (1997), katabatic winds dominate over the Antarctic coastal zone, particularly in East Antarctica. However, Massom et al. (1998) stressed the importance of easterlies. Distinguishing between them is not necessarily easy, as the Coriolis force turns the katabatic winds towards easterlies (Ball, 1960), in particular if the slope is not steep or when the airmass is already over a flat ice shelf or ocean surface.

Coastal polynyas also provide a feedback to wind forcing. At least the following mechanisms affect the feedback. First, stratification of the atmospheric boundary layer is typically stable over sea ice but unstable over polynyas, as the sea surface is typically much warmer than the air above. This leads to stronger turbulent mixing, and therefore to an enhanced vertical momentum flux, which increases near-surface winds (Vihma, 1995; Stössel et al., 2008). Second, this effect is typically enhanced by baroclinicity (Joffre, 1982), as there is a horizontal temperature gradient between the colder air over the ice

sheet or ice shelf and a heated air over the open water. Third, the near-surface winds over the polynya may be strengthened by a mesoscale sea breeze or land breeze, depending on the season (Kottmeier and Engelbart, 1992; Savijärvi, 2011). Fourth, differences in aerodynamic surface roughness between the upwind surface and the polynya result in acceleration of wind over the polynya, which is strongest if the upwind surface is rugged terrain of glaciers and nunataks (Zhang et al., 2015). Deceleration occurs, if the aerodynamic roughness of the upwind surface (e.g. smooth ice shelf) is smaller than that of the polynya. For combined effects of the physical mechanisms related to roughness and stratification, see Jakobson et al. (2019).

2.1.3 Atmospheric circulations over the Southern Ocean

In addition to the katabatic forcing, the wind over coastal polynyas is controlled by mesoscale (Renfrew, 2002; Pezza et al., 2016) and synoptic-scale (Zwally et al., 1985; Jacobs and Comiso, 1989; Uotila et al., 2011) events in the atmospheric pressure patterns over the Southern Ocean and the Antarctic coastal zone. Meso- or synoptic-scale wind vectors, which are oriented along the katabatic wind vectors, provide favorable conditions for the formation of a coastal polynya (Bromwich et al., 1998). In addition to formation of polynyas, synoptic-scale winds affect their evolution. For example, the model experiments of Stössel et al. (2011) suggested that eastward propagation of synoptic-scale cyclones in the Antarctic coastal zone resulted in eastward extension of coastal polynyas.

The cyclone tracks and associated synoptic-scale winds over the Southern Ocean are strongly controlled by larger-scale pressure patterns related to SAM, ENSO, the Amundsen Sea Low (ASL), the Zonal Wave 3 (ZW3), the Antarctic Circumpolar Wave (ACW), and the Semiannual Oscillation (SAO) (Bromwich et al., 1998; Gordon et al., 2007; Uotila et al., 2013; Campagne et al., 2015; Ward, 2018). Among them, at least SAM, ENSO, ASL and ACW have been found to affect the occurrence or size of coastal polynyas.

The influence of SAM on Antarctic sea ice is well known, and strongest in East Antarctica (Simpkins et al., 2012; Raphael and Hobbs, 2014; Zhang et al., 2017). However, in a study addressing 13 coastal polynyas, Tamura et al. (2016) found statistically insignificant correlations between SAM and SIP in the coastal polynyas. According to Ward (2018), this may be due to the fact that Tamura et al. (2016) analyzed annual cumulative sea ice extent. Ward (2018) found strong relationships between SAM and monthly polynya size in East Antarctica: The positive phase of SAM favors smaller polynyas than the negative phase. This is related to the fact that most East Antarctic polynyas grow in size during easterly winds (Nihashi and Ohshima, 2015). Further, Park et al. (2018) suggested an influence of SAM in long-term evolution of the Ross Ice Shelf Polynya (RISP).

ENSO is strongly associated with cyclogenesis and cyclone tracks in the Amundsen and Ross seas, but not much in other parts of the Southern Ocean (Uotila et al., 2013). Hence, it is understandable that the effects of ENSO on coastal polynyas are strongest in the Amundsen and western Ross seas (Bromwich et al., 1998; Tamura et al., 2016; Ward, 2018). Outside of the Amundsen and Ross seas, Marshall and King (1998) have suggested that the persistency of anomalously large Ronne Polynya in summer 1998 was possibly due to the impact of ENSO. Further, Tamura et al. (2016) detected a statistically significant relationship between ENSO and a coastal polynya in the Prydz Bay. In general, there is weak inter-annual variability in the polynya size except for the Weddell, Bellingshausen, and eastern Amundsen seas (Ward, 2018). In the Weddell Sea, only the polynya event occurring in January–February 1998 off the Ronne Ice Shelf could be associated with a circulation pattern induced by ENSO (Ackley et al., 2001). However, in the latter two seas, the inter-annual variability of polynyas is related to the large role of ENSO, which varies a lot inter-annually (Tamura et al., 2016; Park et al., 2018; Ward, 2018). In other parts of the Southern Ocean, the effects of SAM and ASL generate substantial monthly and seasonal variability, whereas the daily peak is due to variability of local synoptic and katabatic winds.

Considering ASL, Ward (2018) found that the latitude, longitude as well as the actual and relative central pressure of ASL all affect the occurrence and size of coastal polynyas in the Amundsen, Bellingshausen and eastern Ross seas. Related to the effects of the cyclonic circulation on sea ice (Turner et al., 2013), the correlation between polynya size and ASL usually had an opposite sign to the east and west of the center of ASL (Ward, 2018). Further, ACW may have affected variations in the formation and persistence of polynyas in the Weddell Sea (White and Peterson, 1996). However, ACW has not received much attention in recent years.

2.2 Sea ice production in coastal polynyas

The major coastal polynyas produce 10% of new ice in the Southern Ocean, though the total coastal polynya area accounts for only about 1% of the maximum sea ice area (Tamura et al., 2008). SIP in coastal polynyas is often estimated by satellite observations in combination with reanalysis of surface heat fluxes, due to the difficulties in taking long-term in-situ observations (Martin, 2004b; Tamura et al., 2007, 2008, 2011; Comiso et al., 2011; Iwamoto et al., 2014). As shown in Figure 1, Tamura et al. (2008) calculated SIP in the Antarctic coastal polynyas by using ice thickness data and heat flux products. The mean values of annual cumulative SIP for the major 13 Antarctic coastal polynyas are shown in Table 1. They revealed that the RISP is the region with the highest SIP around Antarctica, which is consistent with the fact that the Ross Sea is one of the major formation sites of AABW. The area of the RISP was decreased by about 30% from the 1990s to the 2000s. However, SIP in the Weddell Sea, which is also

known as one of the major source regions of AABW (Orsi et al., 2002), is underestimated because the coastal polynyas along the Weddell Sea are difficult to detect due to their narrowness. The second highest SIP occurs in the Cape Darnley Polynya, which has already been proved as the main source of AABW (Ohshima et al., 2013). The third highest SIP is in the Mertz Polynya, which could produce adequate Dense Shelf Water (DSW) as a portion of the Adélie Land Bottom Water (Rintoul, 2013). A prominent feature in Figure 1 is that almost all of the coastal polynyas along the East Antarctic coastline appear on the western sides of the protruding topography, including peninsulas, fast ice and glacial tongues (Nihashi and Ohshima, 2015). These fundings were further verified by analyzing the effects of the Mertz Glacial Tongue calving event in 2010 on the SIP in the Mertz Polynya (Nihashi et al., 2017)

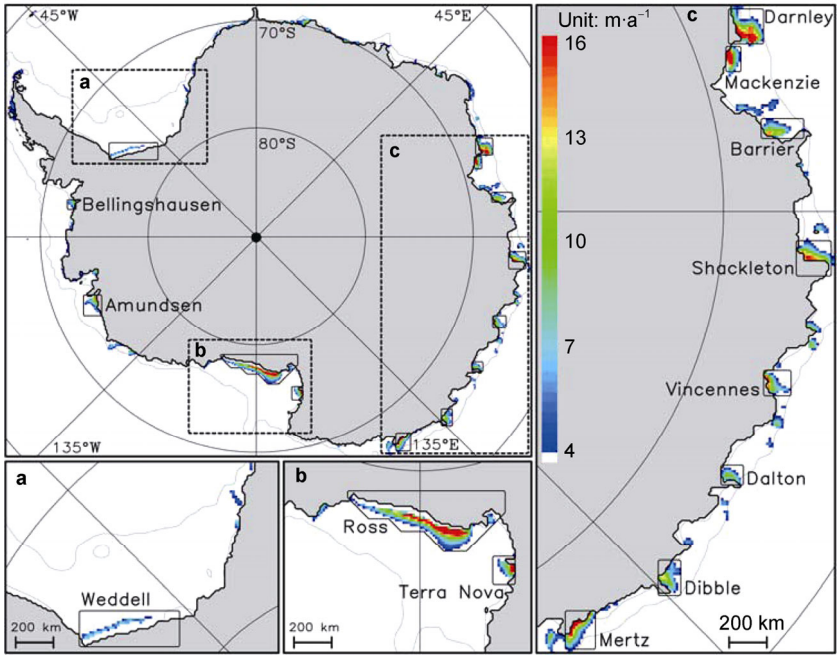

Figure 1 Spatial distribution of annual cumulative SIP averaged over 1992–2001 calculated using the ERA-40 reanalysis product. The Weddell Sea (**a**), Ross Sea (**b**) and East Antarctica (**c**) are enlarged. The 200-m and 1000-m isobaths are indicated by thin lines (Tamura et al., 2008). Figure reuse permission is obtained from the Copyright Clearance Center.

Table 1 Mean values of annual cumulative SIP for the major 13 Antarctic coastal polynyas with their standard deviations and trends (Tamura et al., 2008)

Polynya	SIP/km^3	Trend/(km^3·(10 a)$^{-1}$)
Ross	390±59	−85
Darnley	181±19	−13
Mertz	120±11	+27
Shackleton	110±14	+11
Amundsen	92.0±16	−16
Weddell	84.6±25	−30
Barrier	80.0±19	+44
Dibble	75.5±11	+19
Vincennes	73.3±9.9	+7.7
Mackenzie	68.2±5.8	−7.8
Terra Nova	59.2±10	−3.7
Dalton	42.6±6.7	+1.7
Bellingshausen	33.7±6.1	−7.7
Total	1410±75	−53

Note: Table reuse permission is obtained from the Copyright Clearance Center.

The uncertainties in ice thickness data and surface heat flux data introduce errors to the estimate of SIP. Heat loss at the surface of thin ice is one of the error sources, because the treatment of relatively large short-wave radiation absorbed into the interior ice is uncertain (Tamura et al., 2008). Recent studies have shown that the accuracy of the SIP estimate depends on the types of thin ice areas (Nakata et al., 2019, 2021). Nakata et al. (2021) developed a method to identify the sea ice types from microwave data and divided them into two types — active frazil and thin solid ice, which determine the algorithm of estimating SIP. Applying this new method, the estimated SIP in coastal polynyas along East Antarctica is about 20% to 50% higher than previous estimation, where sea ice is mostly in the form of active frazil ice (Ciappa and Pietranera, 2013; Nakata et al., 2015; Haumann et al., 2020). Although the developed algorithms should have improved the accuracy of the SIP estimation, it is still difficult to analyze the exact error due to the inaccuracy of atmospheric reanalysis products and the lack of in-situ data. At the same time, snow will have an impact on the microwave properties of sea ice and calculation of heat

fluxes, which makes the algorithms not applicable in the case of snow fall. In the future, more in-situ observations will be applied to improving the estimate of SIP. For example, the moored Acoustic Doppler Current Profiler can be used to detect the draft of floating ice and the depth of suspended frazil ice (Fukamachi et al., 2009). Data observed by Ice Profiling Sonar can also be used to calculate the ice thickness and identify the formation of frazil ice, which improves our understanding of the processes controlling SIP in polynyas (Fukamachi et al., 2006; Ito et al., 2015).

2.3 Temporal variations of sea ice and oceanic processes in coastal polynyas

2.3.1 Synoptic scale

Wind and air temperature are the two most important factors affecting the variation of coastal polynyas on synoptic scale. Based on remote sensing data, Dale et al. (2017) found that sea ice concentration (SIC) and sea ice motion had large anomalies during a strong wind event in the Ross Sea Polynya, and the strongest negative correlation between SIC and wind speed occurred when the SIC change lagged wind change by 12 h. The SIC anomalies could continue over a time period greater than the duration of sea ice motion anomalies and strong wind events, indicating that sea ice formation within coastal polynyas occurs through both thermodynamic and dynamic processes. Cheng et al. (2019) estimated SIP from passive microwave SIC images based on a thermodynamic model, and illustrated that about 68% variation of SIP is associated with the wind variation in the RISP. Ding et al. (2020) investigated the relationship between the area of the TNBP and the air temperature as well as different components of wind using the ERA5 reanalysis product. They found that significant correlation between wind speed and the polynya area existed for almost all air temperature intervals, and particularly for higher temperatures. In the low temperature interval of −30°C to −20°C, the polynya area is more correlated with air temperature than with the eastward and northward wind speed. Wenta and Cassano (2020) found that during an extreme katabatic wind event associated with the passage of a cyclone, the wind speed varied from a few meters per second to more than 35 $m \cdot s^{-1}$, and the extent of the TNBP changed from several tens of square kilometers to more than 2000 km^2. Based on hydrography measurements from an austral fall cruise of the Polynyas, Ice Production, and seasonal Evolution in the Ross Sea (PIPERS) program, Thompson et al. (2020) revealed that the short-term ice production rate could be up to 110 $cm \cdot d^{-1}$ during katabatic wind events, compared to the seasonal average value of 29 $cm \cdot d^{-1}$, indicating that the frazil ice production rates (the main component of the total polynya ice production) are strongly correlated with the wind speed.

2.3.2 Seasonal scale

By applying a long-term multiple spatial smoothing method to satellite retrieved SIC data, Jiang et al. (2020) obtained stable annual SIC products and studied the seasonal variations of Antarctic coastal polynya extent. The polynya extent gradually decreases from April to August and then increases from September afterwards. Seasonal variations of water mass properties are also revealed in a few coastal polynyas from mooring observations. Rusciano et al. (2013) found that in the TNBP, HSSW is mainly formed from July to November, while SIP and brine rejection are also active from March to June but do not result in HSSW formation. Yoon et al. (2020) showed that the near-bottom salinity in the TNBP begins to increase in September and decrease in January. The salinity in the western part of TNB increases first from July to September, which is about two months earlier than the salinity increase in the eastern part of TNB.

2.3.3 Interannual scale and long-term trends

Carrying out long-term in-situ observations of coastal polynyas is difficult, and there are only limited works based on satellite remote sensing data that analyzed the variations of sea ice parameters of coastal polynyas on the interannual scale or above. Tamura et al. (2016) found that for most Antarctic coastal polynyas, the interannual variation of SIP is more correlated with the polynya extent than with atmospheric forcing, with the exception being the Shackleton Polynya. The interannual variability in SIP does not show a coherent signal in the major coastal polynya surrounding Antarctica, and is only weakly correlated with SAM or the Southern Oscillation Index (Tamura et al., 2016). The variation of icescapes, such as ice shelves, floating glaciers, fast ice and offshore first-year ice, can affect the interannual variability of SIP in coastal polynyas and their relationship with large-scale climate modes.

For the long-term trends of coastal polynyas, Tamura et al. (2016) found that SIP values in both the RISP and the Mertz Glacier Polynya are reduced, as a result of ice sheet calving events and changes in the location of icebergs and fast ice. On the contrary, Comiso et al. (2011) estimated the SIP in the RISP from 1992 to 2008 year by year by using temperature brightness data, and found that SIP increased over the 17-year period. Drucker et al. (2011) quantified SIP in the Ross Sea, which has a statistically significant positive trend of about 21 $km^3 \cdot a^{-1}$. These different results suggest that the SIP trend estimates need to be validated by long-term in-situ observations of ice properties in Antarctic coastal polynyas, including ship observations and salinity data from moorings. Charrassin et al. (2008) estimated SIP by using salt budget for the upper 100 m of the water column. Nevertheless, the SIP can be underestimated due to the freshening by net precipitation but the seasonal variability of the SIP can be expressed to a certain extent. Tamura et al. (2016) compared the SIP obtained from a heat flux calculation method with satellite-derived thin ice thickness data and atmospheric forcing to the SIP by using salt budget calculation based on Charrassin et al. (2008), and found a good relationship between the broad magnitude

and intramonthly variability of these two independent measurements.

2.4 Role of coastal polynyas on the AABW formation

Based on numerical simulations, Kusahara et al. (2010) quantified the volume fluxes of DSW along East Antarctica (Figure 2) according to different potential density thresholds (Table 2) and the maximum possible formation rate of AABW (Table 3). Kusahara et al. (2011a) evaluated the impact of the Mertz Glacier Tongue calving, which occurred on 12–13 February 2010, on dense water formation and export.

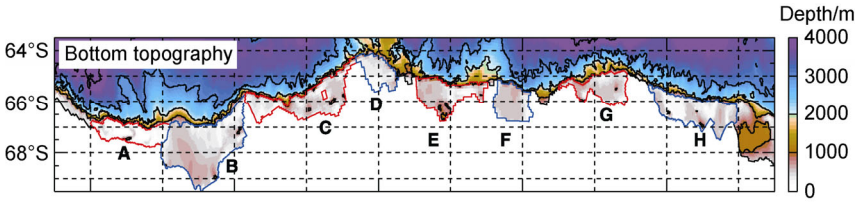

Figure 2 Bottom topography of the model in East Antarctica and control volumes used for the calculation of SIP (A–H, red and blue bounded regions) (Kusahara et al., 2010). Figure reuse permission is obtained from the Copyright Clearance Center.

Table 2 DSW formation in the control volumes A–H[1] that includes the blocking of sea ice advection by grounded icebergs based on different threshold density[2] (Kusahara et al., 2010)

Control volume	Threshold density σ_{th} /(kg·m^{-3})	Formation rate σ_θ >σ_{th}/Sv	Mean density of outflow /(kg·m^{-3})
A	27.78	1.11±0.19	27.933
		0.55±0.18 (North)	27.988 (North)
B	27.68	0.87±0.18	27.789
C	27.66	0.91±0.28	27.765
D	27.68	0.10±0.07	27.776
E	27.70	0.59±0.19	27.808
F	27.64	0.35±0.11	27.770
G	27.62	0.56±0.18	27.744
H	27.78	0.87±0.12	27.854

Notes: [1] The names of control volumes and coastal polynyas are shown in Figure 2a;
[2] For the control volume A, the formation rate and mean density of DSW across the northern boundary are also listed.
Table reuse permission is obtained from the Copyright Clearance Center.

Table 3 Maximum possible formation rates of AABW in the control volumes A–H[1] (Kusahara et al., 2010)

Control volume	$\gamma^n > 28.27$ & $\theta < 0.0$/Sv	$\gamma^n > 28.30$ & $\theta < 0.0$/Sv
A	2.13±0.61	1.97±0.51
B	1.29±0.53	1.05±0.32
C	0.59±0.20	0.45±0.11
D	0.18±0.07	0.15±0.05
E	0.93±0.31	0.71±0.17
F	0.27±0.11	0.20±0.05
G	0.22±0.07	0.16±0.03
H	1.97±0.61	1.64±0.41
Total	7.58	6.33

Notes: [1] The names of control volumes and coastal polynyas are shown in Figure 2a.
Table reuse permission is obtained from the Copyright Clearance Center.

Kusahara et al. (2017) conducted extensive passive tracer experiments and verified nine routes of DSW over the bottom topography of the Southern Ocean because the spatial distribution of nine tracers resembles the AABW distribution. About 50% of the total tracer is transported northward from the continental shelf to the deep ocean, and about 7% is transported poleward beneath ice shelf cavities. Mathiot et al. (2012) employed two different atmospheric forcing sets—DFS3 based on ERA40 as well as satellite products and MAR (Modèle Atmosphérique Régional) based on ERA40 with a dynamical downscaling procedure in a regional ocean-sea-ice circulation model. Compared with DFS3, the local strong katabatic winds along the coast are better represented in MAR. Model simulations forced by MAR with stronger katabatic winds produce a greater flow of dense water exported from the polynyas, and improve the HSSW properties compared with DFS3 forcing. They detected a lag between the time when polynyas were most active over the Ross Shelf and the time when the export of HSSW reached maxima. Barthélemy et al. (2012) corrected the katabatic winds and polar easterlies based on comparison of coastal winds in the ERA40 atmospheric reanalysis with that simulated by the regional model MAR (Mathiot et al., 2010). The correction for katabatic winds reduces the mean errors of deep ocean temperature and salinity by 9% and 37%, respectively, which makes the simulation of AABW more accurate. Stössel et al. (2011) employed two real-time wind datasets (the European Centre for Medium-Range Weather Forecasts, ECMWF) optional analyses and the National Center for Environmental Predictions/National Center for Atmospheric Research (NCEP/NCAR) reanalysis) with different resolutions (about 20 km in ECMWF and 200 km in NCEP/NCAR) to force a Southern Ocean ocean-sea-ice model. Along the coast of the Weddell Sea, SIP produced by the higher-resolution wind forcing almost tripled the values of SIP produced by the lower-resolution wind forcing, and the AABW formation is enhanced. Nevertheless, the SIP forced by the low-resolution product along East Antarctica is higher than that forced by the high-resolution product because of the overestimated offshore wind component in the low-resolution NCEP/NCAR reanalysis. The Antarctic Circumpolar Current (ACC) in the model forced by NCEP/NCAR is about 10% enhanced than that in the model forced by ECMWF. Zhang et al. (2015) evaluated the effects of wind fields from two different operational analyses—ECMWF and the Antarctic Mesoscale Prediction System (AMPS) with similar resolutions on the simulation of coastal polynyas. They showed that AMPS overestimates the coastal wind speed, which results in larger SIP values in coastal polynyas, particularly along the coast of East Antarctica as shown in Figure 3. Wind from ECMWF is in better agreement with data from Antarctic weather stations and produces a more realistic simulation of SIP in the coastal polynyas.

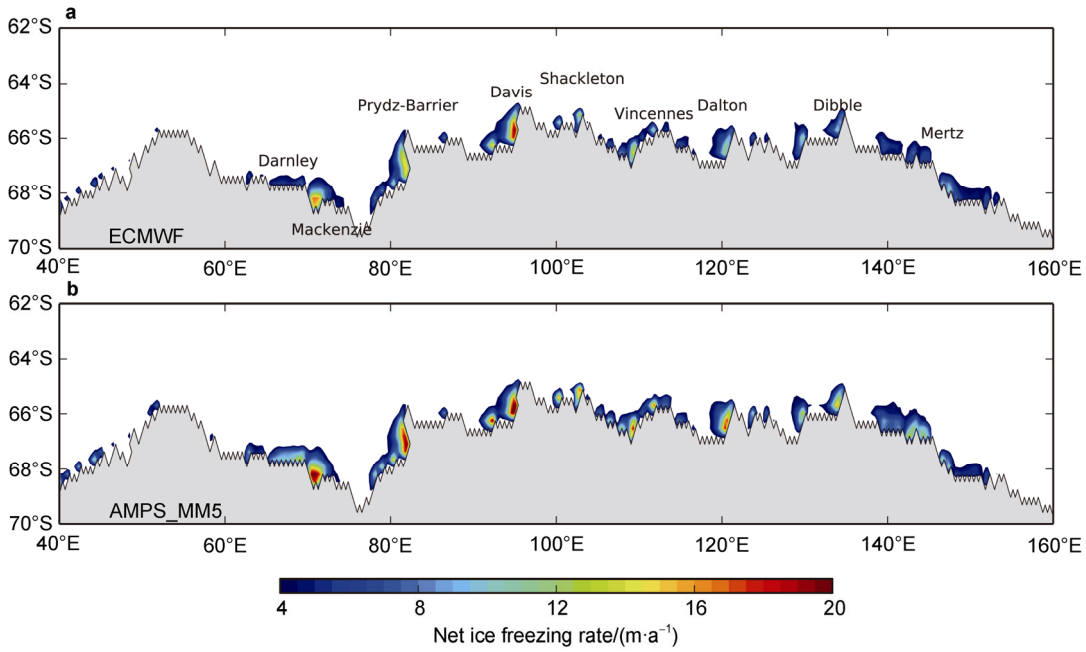

Figure 3 Annual net ice freezing rate for the ECMWF (**a**) and AMPS_MM5 (**b**) simulations in the Darnley, Mackenzie, Prydz-Barrier, Davis, Shackleton, Vincennes, Dalton, Dibble and Mertz glacier polynyas along the East Antarctic coast. Above polynyas are labeled in panel (**a**) (Zhang et al., 2015). Figure reuse permission is obtained from the Copyright Clearance Center.

3 Open-ocean polynyas

Two major open-ocean polynyas in the Southern Ocean have been observed for the first time since satellite observation techniques were first used to observe winter sea ice in 1972. Applying the Nimbus 5 Electrically Scanning

Microwave Radiometer data, Carsey (1980) detected a persistent large-scale open-ocean polynya, which is known as the WP. The averaged area of WP was estimated to reach 2.5×10^5 km^2 (Gordon et al., 2007). However, it is not a recurring open-ocean polynya, and opened successively in the three winters from 1974 to 1976, developing from its precursor — the MRP, formed near the Maud Rise in the Weddell Sea during late winter and early spring in 1973 (Comiso and Gordon, 1987). Nevertheless, not every MRP event could generate a WP event. While the MRP event occurring in austral autumn of 2016 was also a precursor to the following WP event in 2017, the largest MRP event since 1980, which occurred in 2017, did not generate a WP event in 2018 (Cheon and Gordon, 2019). Qian et al. (2020) analyzed the temporal variation characteristics of the MRP (1973, 1980–2017) and the WP (1974–1976) based on the SIC data derived from the Advanced Microwave Scanning Radiometer-2. They found that the WP lasted from the freezing to melting seasons, while the MRP appeared later and lasted for 3 d to 23 d (except for more than 90 d in 2017), which reflected the large differences in oceanic convective activities between the two polynyas. WP imposes a significant influence on large-scale oceanic processes, such as the mid-depth cooling induced by deep convection (Wang et al., 2017). At the same time, WP has a profound impact on the regional air-sea interaction. In the WP region, the ocean heat loss was estimated to be 100–200 W·m^{-2} in the mid-1970s (Moore et al., 2002). The occurrence of open-ocean polynyas has potential impacts not only on the physical processes in the ocean and atmosphere, but also on the regional primary production and carbon uptake of the Southern Ocean (Bernardello et al., 2014). In 2017, there was an unprecedented phytoplankton bloom in the MRP, which contributed largely to the carbon fixation in this area (Jena and Pillai, 2020).

Another prominent open-ocean polynya appears in the west Cosmonaut Sea, which is known as the west Cosmonaut Sea Polynya (wCSP). wCSP was firstly discovered in 1987 by the scanning multichannel microwave radiometer carried on the Nimbus 7 satellite (Comiso and Gordon, 1987). Unlike the WP, the wCSP can successively reoccur in late autumn and early winter, but the location varies from year to year. The formation of wCSP is closely related to its precursor — the sea ice embayment, which is an open water body surrounded by sea ice on three sides, and the surface area of the sea ice embayment shows an obvious periodicity of three years (Geddes and Moore, 2007).

3.1 The driving force of open-ocean polynyas

3.1.1 Atmospheric forcing

Cheon et al. (2014) proposed that negative wind stress curl formed by the easterlies/katabatic winds and westerlies could enhance deep warm water upwelling and accelerate the formation of WP in the Weddell Sea as shown in Figure 4. Wang et al. (2019) put forward that the sea ice drift anomalies driven by winds in 2016 were mainly responsible for the decreased sea ice extent compared with the warmest ocean surface state generated by strong wind forcing from April to December of 2016 by analyzing a high-resolution, global ocean-sea-ice model. The rapidly decreased sea ice extent around the entire Antarctic between 2014 and 2016 might play a role in the formation of the MRP in 2016. Hirabara et al. (2012) suggested two significant atmospheric factors which caused the formation of WP after no-WP winters based on numerical simulations of a WP event in the 1950s: enhancement of cyclonic activities generating the divergent sea ice anomaly; cooling of the surface air in early winter. At the same time, they also found that the heat loss by the turbulent heat flux in the model would be reduced by prescribed warm surface air temperature, which would then weaken the deep convection and lead to the absence of WP events. Prasad and McClean (2005) carried out idealized numerical experiments to study the formation and evolution of wCSP occurring from May to July 1999. They changed parameters in the model, such as wind speed, wind direction and the sea ice dynamic module, to investigate how different physical processes affect the formation and maintenance of the wCSP, which develops from an embayment surrounded by sea ice on three sides to a polynya as shown in Figure 5. The upward heat flux in the wCSP increased from 5 to 94 W·m^{-2} triggered by the passage of the first storm event on 12–19 June in 1999. Compared with the upward heat flux following the first storm event, the upward heat flux following a weaker wind event that took place on 30 June to 10 July was 65 W·m^{-2}, which had less impact on the embayment area. Bailey (2004) showed that the wCSP was initiated and largely influenced by mesoscale atmospheric divergence events, which is different from the typical open-ocean polynya in the Weddell Sea. However, the simulated wCSP in their model could not be maintained for 6 d but existed for shorter periods than observed because of the lack of an interactive ocean module in the model. In addition to the underestimated duration in models, the observed approximate 3-year periodic variation of wCSP can be neither well simulated nor explained (Geddes and Moore, 2007). Zwally et al. (2002) pointed out that most of the Antarctic sea ice cover presents an interannual variability of about 3–5 a. Such periodic variability may be related to the ACW (White and Peterson, 1996), but Connolley (2002) pointed out that this signal is only visible between 1985 and 1994.

3.1.2 Oceanic forcing

Different from coastal polynyas, the WP is formed mainly due to convection processes which bring warm deep water to the surface layer (Mohrmann et al., 2021). Cheon et al. (2015) argued that the upwelling of the relatively high-salinity Weddell Deep Water (WDW), the increased ice-to-ocean salt flux (i.e., brine injection) and surface

cooling further perturbated the underlying water column, which promoted the open-ocean convection. However, the deep convection is not a sufficient condition for the formation of WP and intermittent WP requires reduced convection to build up a deep heat reservoir (Dufour et al., 2017). The heat supplied from deep layers slows the rate of sea ice freezing and prevents sea ice formation, which promotes the formation of WP (Goosse and Fichefet, 2016). Based on numerical simulations of a WP event in the 1950s, Hirabara et al. (2012) summarized two oceanic factors which favored the formation of the WP after no-WP winters: enhanced potential instability caused by the warmer and saltier deep water transported by advection and eddies; positive salinity anomaly triggered by deep convection that occurred in the preceding winter.

In addition to the physical mechanisms mentioned above, topography also plays an important role in the formation of open-ocean polynyas. Numerical studies reveal that topography can affect polynyas by the Taylor cap circulations over seamounts, trapped and lee waves (Haidvogel et al., 1993), eddy shedding (Holland, 2001), and tidal currents. However, the contribution of the above effects to sea ice divergence remains to be studied in detail (Lindsay et al., 2004). The formation of the MRP, which is smaller than the WP, is related to the Maud Rise seamount. Kurtakoti et al. (2018) successfully explained how the MRP formed by using a high-resolution (0.1° in the ocean component) Earth System Model simulation. The high model resolution enabled more realistic representation of the steep flanks of the rugged topography of and around the Maud Rise, which enabled simulation of a sufficiently strong Taylor column, promoting the formation of the MRP. Even more interesting, the formation of MRP shows multi-decadal variability possibly related to the Southern Ocean Mode (Le Bars et al., 2016), as suggested by modelling studies described in Section 3.2. The above processes are summarized and illustrated in Figure 4 given by Cheon and Gordon (2019).

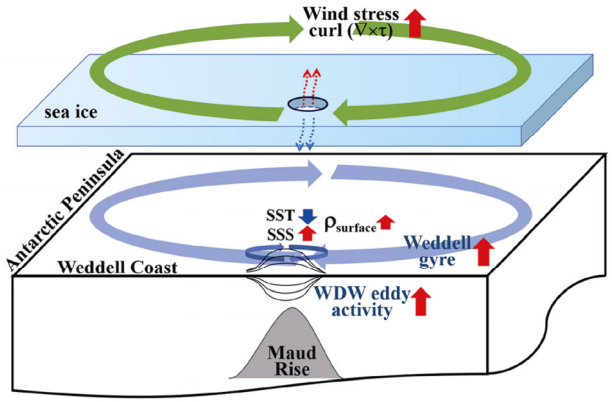

Figure 4 A simple schematic diagram illustrating how an open-ocean polynya is triggered by both hydrological and dynamical processes (Cheon and Gordon, 2019). Figure reuse permission is obtained from the Copyright Clearance Center.

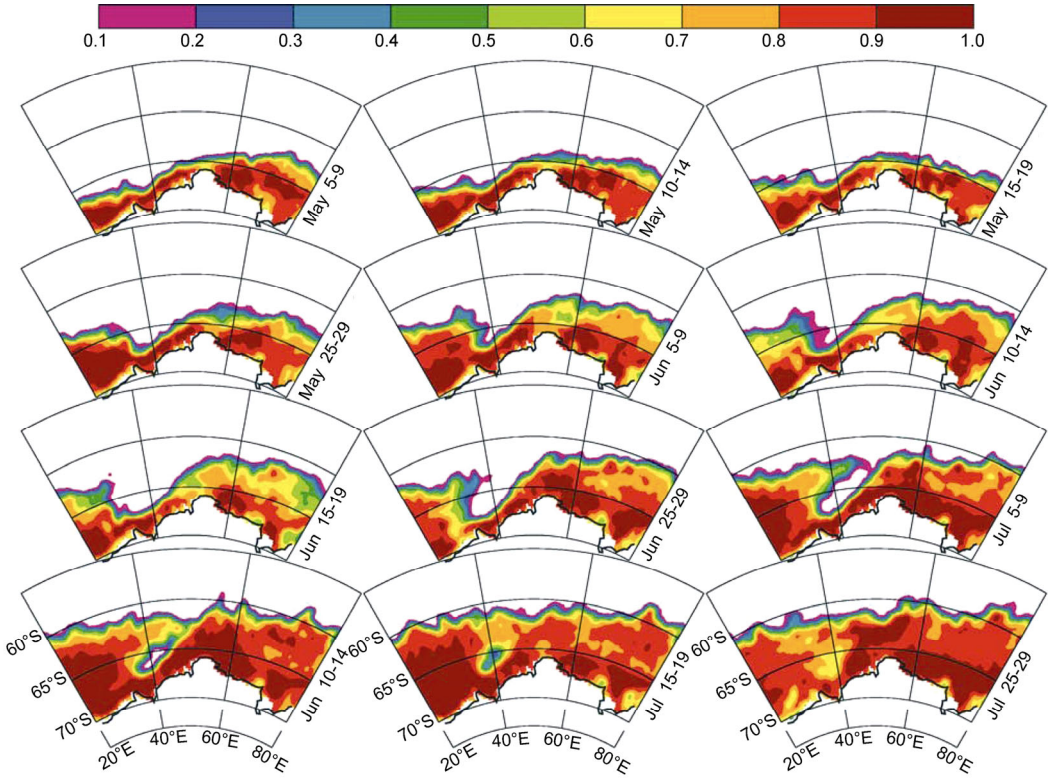

Figure 5 SSM/I-derived SIC (100% = 1) for the Cosmonaut Sea region showing the Cosmonaut Polynya in 1999, which is preceded by an embayment during May–July 1999. These maps are averaged for selected 5-day periods: 5–9, 10–14, 15–19, and 25–29 May (Prasad et al., 2005). Figure reuse permission is obtained from the Copyright Clearance Center.

3.2 The linkage of open-ocean polynyas to climate modes

As mentioned above, the formation of open-ocean polynyas is closely related to atmospheric conditions, such as divergent wind fields, wind speed, surface air temperature and humidity (Gordon et al., 2007). SAM, which is the dominant mode for the climate variability of the Southern Hemisphere extratropical regions, has been shown to have a direct influence on the variability of open-ocean polynyas. The shift of SAM towards its positive phase will result in an increase in the strength of the westerlies and a southward shift of the principal axis of the westerlies (Marshall, 2003; Sen Gupta and England, 2006), and is also associated with increase in the intensity of polar cyclones (Uotila et al., 2013). Numerical experiments conducted by Cheon et al. (2014) increased the strength of westerlies by 20%, which represented the stronger westerlies existing in the mid-1970s following long period of weaker westerlies from 1954 to 1972. The stronger westerlies resulted in a strengthening of the cyclonic Weddell gyre and caused relatively warm WDW to upwell into the surface layer, which melted the sea ice and prevented the formation of new ice, leading to the formation of the WP. Francis et al. (2019) demonstrated that the unprecedented MRP event in mid-September 2017 was caused by the dynamic forcing of cyclonic activities. In addition, SAM can also affect the open-ocean polynyas by influencing air humidity. An analysis of observational data by Gordon et al. (2007) shows that the air was colder and drier than normal when SAM stayed in a prolonged negative phase in the 1970s. The drier air inhibits regional precipitation and increases sea surface salinity, which will weaken the pycnocline compared with wetter conditions. Meanwhile, negative SAM means more sea ice export from the Weddell Sea into the southern branch of the ACC, resulting in intensified brine rejection and destabilization combined with colder weather conditions. The two processes mentioned above associated with a negative SAM phase both promoted the formation of the WP in the 1970s. In contrast, the positive SAM in 2018 resulted in warmer and wetter conditions over the Weddell Sea, which reduced salinity in the surface ocean and inhibited the occurrence of the WP (Cheon and Gordon, 2019). In the future, the SAM index may continue to increase as the greenhouse gas concentrations increase (Thompson and Wallace, 2000; Thompson and Solomon, 2002; Zheng et al., 2013). The strengthening and poleward shift of westerlies will produce stronger negative wind stress curl over the Weddell Sea and accelerate the upwelling of WDW near the Maud Rise, which increases the possibility of the WP formation. Meanwhile, de Lavergne et al. (2014) showed that deep convection has been weakened by surface freshening as SAM progresses towards its positive phase predicted by the Coupled Model Intercomparison Project Phase 5 (CMIP5) models. The ultimate influence of SAM on the formation of open-ocean polynyas and bottom water formation remains unclear and needs to be explored.

In addition to SAM, the tropical climate mode ENSO has also been demonstrated to have significant teleconnection with the climate change in the subpolar regions (Martinson and Iannuzzi, 2003). Many studies have shown that El Niño and La Niña have opposite effects on the Weddell gyre, ocean temperature as well as sea ice cover and formation. La Niña is associated with warmer temperature and less extensive ice cover in the Weddell sector west of the Prime Meridian, and El Niño is associated with colder conditions and large sea ice cover in the western section of the Weddell Sea (Yuan and Martinson, 2000; Kwok and Comiso, 2002). However, the La Niña phase in the mid-1970s caused the slightly colder conditions at the Greenwich Meridian and in the Maud Rise region, which accelerated the formation of sea ice and the destabilization of upper ocean layers (Gordon et al., 2007). In the 1960s, the El Niño phase that preceded the WP formation may have caused the warmer WDW (Robertson et al., 2002; Fahrbach et al., 2004), which increased the possibility of the WP formation. Recent studies have also revealed that an amplification in ZW3, which is associated with the atmospheric anomalies over the Weddell Sea (Raphael, 2004), reached most positive value in the winter of 2017 on record and caused transport of warm air from mid-latitudes to Antarctica (Raphael, 2004; Raphael and Hobbs, 2014). Because of the orographic blocking effect induced by the Antarctic Peninsula, the intrusion of warm and moist air formed an active cyclogenesis zone in the Weddell Sea, which played an important role in the WP event that occurred in the winter of 2017.

4 Remaining challenges

4.1 Lack of knowledge on oceanic forcing

The atmospheric forcing on the occurrence and size of coastal polynyas has received substantial attention, but there is much less quantitative knowledge on the roles of oceanic forcing. On the basis of Arctic observations, it is known that tidal forcing may be important for polynya dynamics in an environment where tides have a strong resonance with the basin geometry. This is the case in parts of the Okhotsk Sea, where the tide-induced mixing affects the vertical heat flux and further winter polynyas (Martin, 2004a). In the Antarctic, only a few studies have quantitatively addressed the effects of tides. Tidal currents are strong, e.g. in the vicinity of the Filchner-Ronne ice front (Robertson et al., 1985; Makinson and Nicholls, 1999), and their effects on polynyas may not be neglected (Morales Maqueda, 2004). Besides tidal currents, the warm, modified CDW, which intrudes onto the continental shelf, will also affect the SIP

in coastal polynyas here (Guo et al., 2019). Considering sea ice, challenges are related to understanding and modelling of frazil ice formation and dynamics, as well as consolidation of frazil ice in the downwind side of coastal polynyas (Ito et al., 2015; Matsumura and Ohshima, 2015; Thompson et al., 2020). For the simulation of the WP, many studies have shown that the open-ocean polynya is over-simulated in models due to the presence of excessive deep convection. The excessive deep convection is triggered by the erosion of stratification in the mixed layer, which is associated with a high salinity bias resulting from insufficient vertical mixing, the lack of freshwater supply from the Antarctic Ice Sheet, or inadequate initial sea ice in the model (Kjellsson et al., 2015; Gutjahr et al., 2019; Held et al., 2019). Based on numerical simulations, Kjellsson et al. (2015) found that the supply of freshwater from the Antarctic Ice Sheet and the initial sea ice conditions play a significant role in the opening of WP. Gutjahr et al. (2019) found that the thicker the sea ice is in the Weddell Sea, the less frequent the occurrence of WP is. Reduced occurrence of WP is also caused by a weaker meridional pressure gradient across the Weddell Sea and the ACC. More accurate simulations of polynyas in the Southern Ocean require increased horizontal resolution, improved vertical discretization schemes, overflow parameterizations and fresh water influxes in the models (Mohrmann et al., 2021).

4.2 Challenges in modelling atmospheric forcing

Modelling of atmospheric forcing on coastal polynyas includes several challenges. The major ones are that coastal polynyas are too small to be well represented by present-day global models and, even for regional high-resolution models and variable-mesh global models, the environment is challenging with complex process interactions between the atmosphere, ocean, sea ice, ice shelves, and land surface (Morales Maqueda, 2004; Petrelli et al., 2008; Mathiot et al., 2012). The local winds over a coastal polynya may include considerable errors and uncertainties due to insufficient representation of the upwind orography and icescape. Important aspects include the shape of the coastline, nunataks, 3D geometry of the ice sheet and glaciers, in particular glacier tongues extending far seaward, and the extent of the ice shelves. If a coastal polynya is located in a site where the small-scale orography generates acceleration of wind (e.g. a seaward-oriented mountain valley upwind of a polynya), too low a resolution in an atmospheric model results in underestimation of winds over a coastal polynya, whereas overestimation occurs if the net effect of the upwind orography is to slow down the winds, e.g. via a ridge of nunataks parallel to the coastline (Stössel et al., 2011; Zhang et al., 2015). Such resolution-related modelling challenges still require a lot of attention, but are expected to reduce with continuous increase in model resolution. For WP, the atmospheric forcing lacking interannual variability causes the simulated polynyas to be more periodic and regular, which is inconsistent with the real situation (Goosse and Fichefet, 2016).

4.3 Lack of knowledge on long-term variability of coastal polynyas under the influence of climate modes

Coupled ocean-sea-ice models are effective tools to study the long-term variability of sea ice, and most of the previous numerical simulations were based on model experiments to explore the long-term variability of sea ice in the coastal polynyas by changing the atmospheric forcing, such as katabatic winds (Mathiot et al., 2010; Barthélemy et al., 2012; Mathiot et al., 2012). Stössel et al. (2011) and Zhang et al. (2015) revealed the influence of representation of orography and parameterizations of subgrid orographic drag in atmospheric reanalysis data on consequent changes of SIP in coastal polynyas, HSSW formation rate, and the intensity of simulated ACC in ocean-sea-ice models. However, the real long-term variability characteristics and driving mechanisms of sea ice and water masses in coastal polynyas are still poorly known. Whether there is a relationship between such variability and climate modes and by which mechanisms the climate modes can influence sea ice and HSSW formation in coastal polynyas are two scientific issues worth of further research.

5 Summary

In this work, observational and modelling studies of the polynyas in the Southern Ocean in recent decades are reviewed. There are two types of polynyas in the Southern Ocean: coastal polynyas and open-ocean polynyas, which are different in formation and maintenance mechanisms. We summarized the formation and maintenance mechanisms, the sea ice production and the water mass formation of the two polynya types, as well as their temporal variations and controlling factors. Studying these processes is important for understanding the regulations of polar climate systems and ecosystems in the Southern Ocean. Ultimately, we proposed challenges in the current polynya research. Lack of knowledge on oceanic forcing and frazil ice dynamics and the difficulties in modelling atmospheric forcing are urgent problems, which directly affect the simulation of polynyas. The solutions of these problems depend on the continuous improvements of configurations, such as horizontal resolution, vertical discretization schemes, overflow parameterizations and fresh water influxes in the models and the observations of polynyas on longer time scales.

Acknowledgements This work is funded by the National Natural Science Foundation of China (Grant nos. 41941008 and 41876221), the Shanghai Science and Technology Committee (Grant nos. 20230711100 and 21QA1404300), the Academy of Finland (Grant no. 304345), the Ministry of Natural Resources of the People's Republic of China (Impact and Response of Antarctic Seas to Climate Change, Grant no. IRASCC

1-02-01B) and the Advanced Polar Science Institute of Shanghai (APSIS). We would like to thank three anonymous reviewers, and Guest Editor Dr. Ruibo Lei for their valuable suggestions and comments that improved this article.

References

Ackley S F, Geiger C A, King J C, et al. 2001. The Ronne Polynya of 1997/98: observations of air-ice-ocean interaction. Ann Glaciol, 33: 425-429, doi:10.3189/172756401781818725.

Adolphs U, Wendler G. 1995. A pilot study on the interactions between katabatic winds and polynyas at the Adélie Coast, eastern Antarctica. Antarct Sci, 7(3): 307-314, doi:10.1017/s0954102095000423.

Alam A, Curry J. 1995. Lead-induced atmospheric circulations. J Geophys Res, 100(C3): 4643-4651, doi:10.1029/94jc02562.

Arbetter T E. 2004. Relationship between synoptic forcing and polynya formation in the Cosmonaut Sea: 1. Polynya climatology. J Geophys Res, 109(C4): C04022, doi:10.1029/2003jc001837.

Arrigo K R. 2003. Phytoplankton dynamics within 37 Antarctic coastal polynya systems. J Geophys Res, 108(C8): 3271, doi:10.1029/2002jc001739.

Arrigo K R, Weiss A M, Smith W O Jr. 1998. Physical forcing of phytoplankton dynamics in the southwestern Ross Sea. J Geophys Res, 103(C1): 1007-1021, doi:10.1029/97jc02326.

Bailey D A. 2004. Relationship between synoptic forcing and polynya formation in the Cosmonaut Sea: 2. Regional climate model simulations. J Geophys Res, 109(C4): C04023, doi:10.1029/2003jc001838.

Ball F K. 1960. Winds on the ice slopes of Antarctica. Antarct Meteorol, 9-16.

Barber D, Marsden R, Minnett P, et al. 2001. Physical processes within the North Water (NOW) Polynya. Atmosphere-Ocean, 39(3): 163-166, doi:10.1080/07055900.2001.9649673.

Barthélemy A, Goosse H, Mathiot P, et al. 2012. Inclusion of a katabatic wind correction in a coarse-resolution global coupled climate model. Ocean Modelling, 48: 45-54, doi:10.1016/j.ocemod.2012.03.002.

Bernardello R, Marinov I, Palter J B, et al. 2014. Impact of Weddell Sea deep convection on natural and anthropogenic carbon in a climate model. Geophys Res Lett, 41(20): 7262-7269, doi:10.1002/2014gl061313.

Blain S, Quéguiner B, Armand L, et al. 2007. Effect of natural iron fertilization on carbon sequestration in the Southern Ocean. Nature, 446(7139): 1070-1074, doi:10.1038/nature05700.

Bromwich D, Liu Z, Rogers A N, et al. 1998. Winter atmospheric forcing of the Ross Sea Polynya//Jacobs S S, Weiss R F. Ocean, ice, and atmosphere: interactions at the Antarctic continental margin. Washington, D. C.: American Geophysical Union, 101-133, doi:10.1029/ar075p0101.

Campagne P, Crosta X, Houssais M N, et al. 2015. Glacial ice and atmospheric forcing on the Mertz Glacier Polynya over the past 250 years. Nat Commun, 6: 6642, doi:10.1038/ncomms7642.

Campbell E C, Wilson E A, Moore G W K, et al. 2019. Antarctic offshore polynyas linked to Southern Hemisphere climate anomalies. Nature, 570(7761): 319-325, doi:10.1038/s41586-019-1294-0.

Carsey F D. 1980. Microwave observation of the Weddell Polynya. Mon Wea Rev, 108(12): 2032-2044, doi:10.1175/1520-0493(1980)108<2032: mootwp>2.0.co;2.

Charrassin J B, Hindell M, Rintoul S R, et al. 2008. Southern Ocean frontal structure and sea-ice formation rates revealed by elephant seals. PNAS, 105(33): 11634-11639, doi:10.1073/pnas.0800790105.

Cheng Z A, Pang X P, Zhao X, et al. 2019. Heat flux sources analysis to the Ross Ice Shelf Polynya ice production time series and the impact of wind forcing. Remote Sens, 11(2): 188, doi:10.3390/rs11020188.

Cheon W G, Gordon A L. 2019. Open-ocean polynyas and deep convection in the Southern Ocean. Sci Rep, 9(1): 1-9, doi:10.1038/s41598-019-43466-2.

Cheon W G, Lee S K, Gordon A L, et al. 2015. Replicating the 1970s' Weddell Polynya using a coupled ocean-sea ice model with reanalysis surface flux fields. Geophys Res Lett, 42(13): 5411-5418, doi:10.1002/2015gl064364.

Cheon W G, Park Y G, Toggweiler J R, et al. 2014. The relationship of Weddell Polynya and open-ocean deep convection to the southern hemisphere westerlies. J Phys Oceanogr, 44(2): 694-713, doi:10.1175/jpo-d-13-0112.1.

Ciappa A, Pietranera L. 2013. High resolution observations of the Terra Nova Bay Polynya using COSMO-SkyMed X-SAR and other satellite imagery. J Mar Syst, 113-114: 42-51, doi:10.1016/j.jmarsys.2012.12.004.

Comiso J C, Gordon A L. 1987. Recurring polynyas over the Cosmonaut Sea and the Maud Rise. J Geophys Res, 92(C3): 2819, doi:10.1029/jc092ic03p02819.

Comiso J C, Gordon A L. 1996. Cosmonaut Polynya in the Southern Ocean: structure and variability. J Geophys Res, 101(C8): 18297-18313, doi:10.1029/96jc01500.

Comiso J C, Kwok R, Martin S, et al. 2011. Variability and trends in sea ice extent and ice production in the Ross Sea. J Geophys Res, 116(C4): C04021, doi:10.1029/2010jc006391.

Connolley W M. 2002. Long-term variation of the Antarctic circumpolar wave. J Geophys Res, 108(C4): 8076, doi:10.1029/2000jc000380.

Dale E R, McDonald A J, Coggins J H J, et al. 2017. Atmospheric forcing of sea ice anomalies in the Ross Sea Polynya region. Cryosphere, 11(1): 267-280, doi:10.5194/tc-11-267-2017.

de Lavergne C, Palter J B, Galbraith E D, et al. 2014. Cessation of deep convection in the open Southern Ocean under anthropogenic climate change. Nat Clim Change, 4(4): 278-282, doi:10.1038/nclimate2132.

Ding Y F, Cheng X, Li X C, et al. 2020. Specific relationship between the surface air temperature and the area of the Terra Nova Bay Polynya, Antarctica. Adv Atmos Sci, 37(5): 532-544, doi:10.1007/s00376-020-9146-2.

Drucker R, Martin S, Kwok R. 2011. Sea ice production and export from coastal polynyas in the Weddell and Ross seas. Geophys Res Lett, 38(17): L17502, doi:10.1029/2011gl048668.

Dufour C O, Morrison A K, Griffies S M, et al. 2017. Preconditioning of the Weddell Sea Polynya by the ocean mesoscale and dense water overflows. J Clim, 30(19): 7719-7737, doi:10.1175/jcli-d-16-0586.1.

Fahrbach E, Hoppema M, Rohardt G, et al. 2004. Decadal-scale variations of water mass properties in the deep Weddell Sea. Ocean Dyn, 54(1): 77-91, doi:10.1007/s10236-003-0082-3.

Francis D, Eayrs C, Cuesta J, et al. 2019. Polar cyclones at the origin of the reoccurrence of the Maud Rise Polynya in austral winter 2017. J Geophys Res Atmos, 124(10): 5251-5267, doi:10.1029/2019jd030618.

Fukamachi Y, Mizuta G, Ohshima K I, et al. 2006. Sea ice thickness in the

southwestern Sea of Okhotsk revealed by a moored ice-profiling sonar. J Geophys Res, 111(C9): C09018, doi:10.1029/2005jc003327.

Fukamachi Y, Shirasawa K, Polomoshnov A M, et al. 2009. Direct observations of sea-ice thickness and brine rejection off Sakhalin in the Sea of Okhotsk. Cont Shelf Res, 29(11-12): 1541-1548, doi:10.1016/j.csr.2009.04.005.

Gallée H. 1997. Air-sea interactions over Terra Nova Bay during winter: simulation with a coupled atmosphere-polynya model. J Geophys Res, 102(D12): 13835-13849, doi:10.1029/96jd03098.

Geddes J A, Moore G W K. 2007. A climatology of sea ice embayments in the Cosmonaut Sea, Antarctica. Geophys Res Lett, 34(2): L02505, doi:10.1029/2006gl027910.

Gilchrist H G, Robertson G J. 2000. Observations of marine birds and mammals wintering at polynyas and ice edges in the Belcher Islands, Nunavut, Canada. Arctic, 53(1): 61-68, doi:10.14430/arctic835.

Goosse H, Fichefet T. 2001. Open-ocean convection and polynya formation in a large-scale ice–ocean model. Tellus A: Dyn Meteorol Oceanogr, 53(1): 94-111, doi:10.3402/tellusa.v53i1.12175.

Gordon A L, Comiso J C. 1988. Polynyas in the Southern Ocean. Sci Am, 258(6): 90-97, doi:10.1038/scientificamerican0688-90.

Gordon A L, Visbeck M, Comiso J C. 2007. A possible link between the Weddell Polynya and the Southern Annular Mode. J Clim, 20(11): 2558-2571, doi:10.1175/jcli4046.1.

Govin A, Michel E, Labeyrie L, et al. 2009. Evidence for northward expansion of Antarctic Bottom Water mass in the Southern Ocean during the last glacial inception. Paleoceanography, 24(1): PA1202, doi:10.1029/2008pa001603.

Guo G J, Shi J X, Gao L B, et al. 2019. Reduced sea ice production due to upwelled oceanic heat flux in Prydz Bay, East Antarctica. Geophys Res Lett, 46(9): 4782-4789, doi:10.1029/2018gl081463.

Gutjahr O, Putrasahan D, Lohmann K, et al. 2019. Max Planck Institute Earth System Model (MPI-ESM1.2) for the High-Resolution Model Intercomparison Project (HighResMIP). Geosci Model Dev, 12(7): 3241-3281, doi:10.5194/gmd-12-3241-2019.

Haidvogel D B, Beckmann A, Chapman D C, et al. 1993. Numerical simulation of flow around a tall isolated seamount. Part II: resonant generation of trapped waves. J Phys Oceanogr, 23(11): 2373-2391, doi:10.1175/1520-0485(1993)023<2373: nsofaa>2.0.co;2.

Haumann F A, Moorman R, Riser S C, et al. 2020. Supercooled Southern Ocean waters. Geophys Res Lett, 47(20): e2020GL090242, doi:10.1029/2020gl090242.

Held I M, Guo H, Adcroft A, et al. 2019. Structure and performance of GFDL's CM4.0 climate model. J Adv Model Earth Syst, 11(11): 3691-3727, doi:10.1029/2019ms001829.

Hirabara M, Tsujino H, Nakano H, et al. 2012. Formation mechanism of the Weddell Sea Polynya and the impact on the global abyssal ocean. J Oceanogr, 68(5): 771-796, doi:10.1007/s10872-012-0139-3.

Holland D M. 2001. Explaining the Weddell Polynya—a large ocean eddy shed at Maud Rise. Science, 292(5522): 1697-1700, doi:10.1126/science.1059322.

Hoppema M, Anderson L G. 2007. Chapter 6 Biogeochemistry of polynyas and their role in sequestration of anthropogenic constituents//Smith W O, Barber D G. Polynyas: windows to the world (Volume 74). Amsterdam: Elsevier, 193-221, doi:10.1016/s0422-9894(06)74006-5.

Ito M, Ohshima K I, Fukamachi Y, et al. 2015. Observations of supercooled water and frazil ice formation in an Arctic coastal polynya from moorings and satellite imagery. Ann Glaciol, 56(69): 307-314, doi:10.3189/2015aog69a839.

Iwamoto K, Ohshima K I, Tamura T. 2014. Improved mapping of sea ice production in the Arctic Ocean using AMSR-E thin ice thickness algorithm. J Geophys Res Oceans, 119(6): 3574-3594, doi:10.1002/2013jc009749.

Jacobs S S. 2004. Bottom water production and its links with the thermohaline circulation. Antarct Sci, 16(4): 427-437, doi:10.1017/s095410200400224x.

Jacobs S S, Comiso J C. 1989. Sea ice and oceanic processes on the Ross Sea continental shelf. J Geophys Res, 94(C12): 18195, doi:10.1029/jc094ic12p18195.

Jakobson L, Vihma T, Jakobson E. 2019. Relationships between sea ice concentration and wind speed over the Arctic Ocean during 1979–2015. J Clim, 32(22): 7783-7796, doi:10.1175/jcli-d-19-0271.1.

Jena B, Pillai A N. 2020. Satellite observations of unprecedented phytoplankton blooms in the Maud Rise Polynya, Southern Ocean. Cryosphere, 14(4): 1385-1398, doi:10.5194/tc-14-1385-2020.

Jiang L Y, Ma Y, Chen F, et al. 2020. Trends in the stability of Antarctic coastal polynyas and the role of topographic forcing factors. Remote Sens, 12(6): 1043, doi:10.3390/rs12061043.

Joffre S M. 1982. Assessment of the separate effects of baroclinicity and thermal stability in the atmospheric boundary layer over the sea. Tellus, 34(6): 567-578, doi:10.1111/j.2153-3490.1982.tb01845.x.

Kern S. 2009. Wintertime Antarctic coastal polynya area: 1992–2008. Geophys Res Lett, 36(14): L14501, doi:10.1029/2009gl038062.

Kitade Y, Shimada K, Tamura T, et al. 2014. Antarctic bottom water production from the Vincennes Bay Polynya, East Antarctica. Geophys Res Lett, 41(10): 3528-3534, doi:10.1002/2014gl059971.

Kjellsson J, Holland P R, Marshall G J, et al. 2015. Model sensitivity of the Weddell and Ross seas, Antarctica, to vertical mixing and freshwater forcing. Ocean Modelling, 94: 141-152, doi:10.1016/j.ocemod.2015.08.003.

Klunder M B, Laan P, de Baar H J W, et al. 2014. Dissolved Fe across the Weddell Sea and Drake Passage: impact of DFe on nutrient uptake. Biogeosciences, 11(3): 651-669, doi:10.5194/bg-11-651-2014.

Kottmeier C, Engelbart D. 1992. Generation and atmospheric heat exchange of coastal polynyas in the Weddell Sea. Bound Layer Meteorol, 60(3): 207-234, doi:10.1007/BF00119376.

Kurtakoti P, Veneziani M, Stössel A, et al. 2018. Preconditioning and formation of Maud Rise Polynyas in a high-resolution earth system model. J Climate, 31(23): 9659-9678, doi:10.1175/jcli-d-18-0392.1.

Kurtz D D, Bromwich D H. 1985. A recurring, atmospherically forced polynya in Terra Nova Bay//Jacobs S. Oceanology of the Antarctic continental shelf. Washington, D. C.: American Geophysical Union, 177-201, doi:10.1029/ar043p0177.

Kusahara K, Hasumi H, Tamura T. 2010. Modeling sea ice production and dense shelf water formation in coastal polynyas around East Antarctica. J Geophys Res, 115(C10): 2010JC006133, doi:10.1029/2010jc006133.

Kusahara K, Hasumi H, Williams G D. 2011a. Dense shelf water formation and brine-driven circulation in the Adélie and George V Land region. Ocean Modelling, 37(3-4): 122-138, doi:10.1016/j.ocemod.2011.01.008.

Kusahara K, Hasumi H, Williams G D. 2011b. Impact of the Mertz Glacier Tongue calving on dense water formation and export. Nat Commun, 2:

159, doi:10.1038/ncomms1156.

Kusahara K, Williams G D, Tamura T, et al. 2017. Dense shelf water spreading from Antarctic coastal polynyas to the deep Southern Ocean: a regional circumpolar model study. J Geophys Res Oceans, 122(8): 6238-6253, doi:10.1002/2017jc012911.

Kwok R, Comiso J C. 2002. Southern Ocean climate and sea ice anomalies associated with the Southern Oscillation. J Climate, 15(5): 487-501, doi:10.1175/1520-0442(2002)015<0487: socasi>2.0.co;2.

Kwok R, Comiso J C, Martin S, et al. 2007. Ross Sea Polynyas: response of ice concentration retrievals to large areas of thin ice. J Geophys Res, 112(C12): C12012, doi:10.1029/2006jc003967.

Lacarra M, Houssais M N, Herbaut C, et al. 2014. Dense shelf water production in the Adélie Depression, East Antarctica, 2004–2012: impact of the Mertz Glacier calving. J Geophys Res Oceans, 119(8): 5203-5220, doi:10.1002/2013jc009124.

Le Bars D, Viebahn J P, Dijkstra H A. 2016. A Southern Ocean mode of multidecadal variability. Geophys Res Lett, 43(5): 2102-2110, doi:10.1002/2016gl068177.

Lebedev V L. 1968. Maximum size of a wind-generated lead during sea freezing. Oceanology, 8: 313-318.

Lindsay R W, Holland D M, Woodgate R A. 2004. Halo of low ice concentration observed over the Maud Rise seamount. Geophys Res Lett, 31(13): L13302, doi:10.1029/2004gl019831.

Makinson K, Nicholls K W. 1999. Modeling tidal currents beneath Filchner-Ronne Ice Shelf and on the adjacent continental shelf: their effect on mixing and transport. J Geophys Res, 104(C6): 13449-13465, doi:10.1029/1999jc900008.

Markus T, Burns B A. 1995. A method to estimate subpixel-scale coastal polynyas with satellite passive microwave data. J Geophys Res, 100(C3): 4473, doi:10.1029/94jc02278.

Marshall G J. 2003. Trends in the Southern Annular Mode from observations and reanalyses. J Climate, 16(24): 4134-4143, doi:10. 1175/1520-0442(2003)016<4134: titsam>2.0.co;2.

Marshall G J, King J C. 1998. Southern hemisphere circulation anomalies associated with extreme Antarctic Peninsula winter temperatures. Geophys Res Lett, 25(13): 2437-2440, doi:10.1029/98gl01651.

Marshall J, Speer K. 2012. Closure of the meridional overturning circulation through Southern Ocean upwelling. Nat Geosci, 5(3): 171-180, doi:10.1038/ngeo1391.

Martin S. 2004a. Estimation of the thin ice thickness and heat flux for the Chukchi Sea Alaskan coast polynya from Special Sensor Microwave/ Imager data, 1990–2001. J Geophys Res, 109(C10): C10012, doi:10. 1029/2004jc002428.

Martin S. 2004b. Okhotsk Sea Kashevarov Bank Polynya: its dependence on diurnal and fortnightly tides and its initial formation. J Geophys Res, 109(C9): C09S04, doi:10.1029/2003jc002215.

Martinson D G, Iannuzzi R A. 2003. Spatial/temporal patterns in Weddell gyre characteristics and their relationship to global climate. J Geophys Res, 108(C4): 8083, doi:10.1029/2000jc000538.

Massom R A, Harris P T, Michael K J, et al. 1998. The distribution and formative processes of latent-heat polynyas in East Antarctica. Ann Glaciol, 27: 420-426, doi:10.3189/1998aog27-1-420-426.

Mathiot P, Barnier B, Gallée H, et al. 2010. Introducing katabatic winds in global ERA40 fields to simulate their impacts on the Southern Ocean and sea-ice. Ocean Modelling, 35(3): 146-160, doi:10.1016/j.ocemod. 2010.07.001.

Mathiot P, Jourdain N C, Barnier B, et al. 2012. Sensitivity of coastal polynyas and high-salinity shelf water production in the Ross Sea, Antarctica, to the atmospheric forcing. Ocean Dyn, 62(5): 701-723, doi:10.1007/s10236-012-0531-y.

Matsumura Y, Ohshima K I. 2015. Lagrangian modelling of frazil ice in the ocean. Ann Glaciol, 56(69): 373-382, doi:10.3189/2015aog69a 657.

Maykut G A. 1978. Energy exchange over young sea ice in the central Arctic. J Geophys Res, 83(C7): 3646, doi:10.1029/jc083ic07p03646.

McMahon C, Hindell M, Dorr T, et al. 2002. Winter distribution and abundance of crabeater seals off George V Land, East Antarctica. Antarct Sci, 14(2): 128-133, doi:10.1017/s0954102002000688.

Miller L A, DiTullio G R. 2007. Chapter 5 Gas fluxes and dynamics in polynyas//Smith W O, Barber D G. Polynyas: windows to the world (Volume 74). Amsterdam: Elsevier, 163-191, doi:10.1016/s0422-9894(06)74005-3.

Mohrmann M, Heuzé C, Swart S. 2021. Southern Ocean polynyas in CMIP6 models. Cryosphere, 15(9): 4281-4313, doi:10.5194/tc-15-4281-2021.

Moore G W K, Alverson K, Renfrew I A. 2002. A reconstruction of the air–sea interaction associated with the Weddell Polynya. J Phys Oceanogr, 32(6): 1685-1698, doi:10.1175/1520-0485(2002)032<1685: arotas>2.0.co;2.

Morales Maqueda M A. 2004. Polynya dynamics: a review of observations and modeling. Rev Geophys, 42: RG1004, doi:10.1029/2002rg000 116.

Mundy C J, Barber D G. 2001. On the relationship between spatial patterns of sea-ice type and the mechanisms which create and maintain the North Water (NOW) polynya. Atmosphere-Ocean, 39(3): 327-341, doi:10.1080/07055900.2001.9649684.

Nakata K, Ohshima K I, Nihashi S, et al. 2015. Variability and ice production budget in the Ross Ice Shelf Polynya based on a simplified polynya model and satellite observations. J Geophys Res Oceans, 120(9): 6234-6252, doi:10.1002/2015jc010894.

Nakata K, Ohshima K I, Nihashi S. 2019. Estimation of thin-ice thickness and discrimination of ice type from AMSR-E passive microwave data. IEEE Trans Geosci Remote Sens, 57(1): 263-276, doi:10.1109/ TGRS.2018.2853590.

Nakata K, Ohshima K I, Nihashi S. 2021. Mapping of active frazil for Antarctic coastal polynyas, with an estimation of sea-ice production. Geophys Res Lett, 48(6): e2020GL091353, doi:10.1029/2020gl091 353.

Naveira Garabato A C, McDonagh E L, Stevens D P, et al. 2002. On the export of Antarctic Bottom Water from the Weddell Sea. Deep Sea Res Part II: Top Stud Oceanogr, 49(21): 4715-4742, doi:10. 1016/S0967-0645(02)00156-X.

Nihashi S, Ohshima K I. 2015. Circumpolar mapping of Antarctic coastal polynyas and landfast sea ice: relationship and variability. J Clim, 28(9): 3650-3670, doi:10.1175/jcli-d-14-00369.1.

Nihashi S, Ohshima K I, Tamura T. 2017. Sea-ice production in Antarctic coastal polynyas estimated from AMSR2 data and its validation using AMSR-E and SSM/I-SSMIS data. IEEE J Sel Top Appl Earth Obs Remote Sens, 10(9): 3912-3922, doi:10.1109/JSTARS.2017.2731995.

NøSt O A, ØSterhus S. Impact of grounded icebergs on the hydrographic conditions near the Filchner Ice Shelf//Jacobs S S, Weiss R F. Ocean, ice, and atmosphere: interactions at the Antarctic continental margin. Washington, D. C.: American Geophysical Union, 267-284. doi:10.

1029/ar075p0267.

Ohshima K I, Fukamachi Y, Williams G D, et al. 2013. Antarctic Bottom Water production by intense sea-ice formation in the Cape Darnley polynya. Nat Geosci, 6(3): 235-240, doi:10.1038/ngeo1738.

Ohshima K I, Nihashi S, Iwamoto K. 2016. Global view of sea-ice production in polynyas and its linkage to dense/bottom water formation. Geosci Lett, 3(1): 1-14, doi:10.1186/s40562-016-0045-4.

Orsi A H, Johnson G C, Bullister J L. 1999. Circulation, mixing, and production of Antarctic Bottom Water. Prog Oceanogr, 43(1): 55-109, doi:10.1016/S0079-6611(99)00004-X.

Orsi A H, Smethie W M, Bullister J L. 2002. On the total input of Antarctic waters to the deep ocean: a preliminary estimate from chlorofluorocarbon measurements. J Geophys Res, 107(C8): 3122. doi:10.1029/2001jc000976.

Park J, Kim H C, Jo Y H, et al. 2018. Multi-temporal variation of the Ross Sea Polynya in response to climate forcings. Polar Res, 37(1): 1444891, doi:10.1080/17518369.2018.1444891.

Pease C H. 1987. The size of wind-driven coastal polynyas. J Geophys Res, 92(C7): 7049-7059, doi:10.1029/jc092ic07p07049.

Petrelli P, Bindoff N L, Bergamasco A. 2008. The sea ice dynamics of Terra Nova Bay and Ross Ice Shelf polynyas during a spring and winter simulation. J Geophys Res, 113(C9): C09003, doi:10.1029/2006jc004048.

Pezza A, Sadler K, Uotila P, et al. 2016. Southern Hemisphere strong polar mesoscale cyclones in high-resolution datasets. Clim Dyn, 47(5-6): 1647-1660, doi:10.1007/s00382-015-2925-2.

Planquette H, Sherrell R M, Stammerjohn S, et al. 2013. Particulate iron delivery to the water column of the Amundsen Sea, Antarctica. Mar Chem, 153: 15-30, doi:10.1016/j.marchem.2013.04.006.

Prasad T G, McClean J L, Hunke E C, et al. 2005. A numerical study of the western Cosmonaut polynya in a coupled ocean-sea ice model. J Geophys Res, 110(C10): C10008, doi:10.1029/2004jc002858.

Qian J C, Wang Z M, Liu C Y, et al. 2020. Characteristics analysis of Weddell Polynya and Maud Rise Polynya from 1972 to 2019, Antarctica. J Meteorol Sci, 40(5): 721-732, doi:10.3969/2020jms.0073 (in Chinese).

Raphael M N. 2004. A zonal wave 3 index for the Southern Hemisphere. Geophys Res Lett, 31(23): L23212, doi:10.1029/2004gl020365.

Raphael M N, Hobbs W. 2014. The influence of the large-scale atmospheric circulation on Antarctic sea ice during ice advance and retreat seasons. Geophys Res Lett, 41(14): 5037-5045, doi:10.1002/2014gl060365.

Renfrew I A. 2002. Coastal polynyas in the southern Weddell Sea: variability of the surface energy budget. J Geophys Res, 107(C6): 3063, doi:10.1029/2000jc000720.

Rintoul S R. 2013. On the origin and influence of Adélie Land bottom water//Jacobs S S, Weiss R F. Ocean, ice, and atmosphere: interactions at the Antarctic continental margin. Washington: American Geophysical Union, 151-171, doi:10.1029/ar075p0151.

Robertson R, Padman L, Egbert G D. 1985. Tides in the Weddell Sea//Jacobs S S, Weiss R F. Ocean, ice, and atmosphere: interactions at the Antarctic continental margin. Washington: American Geophysical Union, 341-369, doi:10.1029/ar075p0341.

Robertson R, Visbeck M, Gordon A L, et al. 2002. Long-term temperature trends in the deep waters of the Weddell Sea. Deep Sea Res Part II: Top Stud Oceanogr, 49(21): 4791-4806, doi:10.1016/S0967-0645(02)00159-5.

Rusciano E, Budillon G, Fusco G, et al. 2013. Evidence of atmosphere-sea ice-ocean coupling in the Terra Nova Bay Polynya (Ross Sea–Antarctica). Cont Shelf Res, 61-62: 112-124, doi:10.1016/j.csr.2013.04.002.

Savijärvi H. 2011. Antarctic local wind dynamics and polynya effects on the Adélie Land coast. Q J Royal Meteorol Soc, 137(660): 1804-1811, doi:10.1002/qj.874.

Sen Gupta A, England M H. 2006. Coupled ocean-atmosphere-ice response to variations in the Southern Annular Mode. J Clim, 19(18): 4457-4486, doi:10.1175/jcli3843.1.

Simpkins G R, Ciasto L M, Thompson D W J, et al. 2012. Seasonal relationships between large-scale climate variability and Antarctic sea ice concentration. J Clim, 25(16): 5451-5469, doi:10.1175/jcli-d-11-00367.1.

Smith S D, Muench R D, Pease C H. 1990. Polynyas and leads: an overview of physical processes and environment. J Geophys Res: Oceans, 95(C6): 9461-9479, doi:10.1029/JC095iC06p09461.

Stössel A, Cheon W G, Vihma T. 2008. Interactive momentum flux forcing over sea ice in a global ocean GCM. J Geophys Res: Oceans, 113(C5): C05010, doi:10.1029/2007JC004173.

Stössel A, Yang K, Kim S J. 2002. On the role of sea ice and convection in a global ocean model. J Phys Oceanogr, 32(4): 1194-1208, doi:10.1175/1520-0485(2002)032<1194: otrosi>2.0.co;2.

Stössel A, Zhang Z R, Vihma T. 2011. The effect of alternative real-time wind forcing on Southern Ocean sea ice simulations. J Geophys Res: Oceans, 116(C11): C11021, doi:10.1029/2011JC007328.

Tamura T, Ohshima K I, Fraser A D, et al. 2016. Sea ice production variability in Antarctic coastal polynyas. J Geophys Res: Oceans, 121(5): 2967-2979, doi:10.1002/2015JC011537.

Tamura T, Ohshima K I, Markus T, et al. 2007. Estimation of thin ice thickness and detection of fast ice from SSM/I data in the Antarctic ocean. J Atmos Ocean Technol, 24(10): 1757-1772, doi:10.1175/jtech2113.1.

Tamura T, Ohshima K I, Nihashi S. 2008. Mapping of sea ice production for Antarctic coastal polynyas. Geophys Res Lett, 35(7): L07606, doi:10.1029/2007GL032903.

Tamura T, Ohshima K I, Nihashi S, et al. 2011. Estimation of surface heat/salt fluxes associated with sea ice growth/melt in the Southern Ocean. SOLA, 7: 17-20, doi:10.2151/sola.2011-005.

Thompson D W J, Solomon S. 2002. Interpretation of recent Southern Hemisphere climate change. Science, 296(5569): 895-899, doi:10.1126/science.1069270.

Thompson D W J, Wallace J M. 2000. Annular modes in the extratropical circulation. Part I: month-to-month variability. J Climate, 13(5): 1000-1016, doi:10.1175/1520-0442(2000)013<1000:amitec>2.0.co;2.

Thompson L, Smith M, Thomson J, et al. 2020. Frazil ice growth and production during katabatic wind events in the Ross Sea, Antarctica. Cryosphere, 14(10): 3329-3347, doi:10.5194/tc-14-3329-2020.

Turner J, Phillips T, Hosking J S, et al. 2013. The Amundsen Sea Low. Int J Climatol, 33(7): 1818-1829, doi:10.1002/joc.3558.

Uotila P, Vihma T, Pezza A B, et al. 2011. Relationships between Antarctic cyclones and surface conditions as derived from high-resolution numerical weather prediction data. J Geophys Res: Atmos, 116(D7): D07109, doi:10.1029/2010JD015358.

Uotila P, Vihma T, Tsukernik M. 2013. Close interactions between the

Antarctic cyclone budget and large-scale atmospheric circulation. Geophys Res Lett, 40(12): 3237-3241, doi:10.1002/grl.50560.

Vihma T. 1995. Subgrid parameterization of surface heat and momentum fluxes over polar oceans. J Geophys Res, 100(C11): 22625, doi:10.1029/95jc02498.

Vihma T, Tuovinen E, Savijärvi H. 2011. Interaction of katabatic winds and near-surface temperatures in the Antarctic. J Geophys Res: Atmos, 116(D21): D21119, doi:10.1029/2010JD014917.

Wang Z M, Turner J, Wu Y, et al. 2019. Rapid decline of total Antarctic sea ice extent during 2014–16 controlled by wind-driven sea ice drift. J Clim, 32(17): 5381-5395, doi:10.1175/jcli-d-18-0635.1.

Wang Z M, Wu Y, Lin X, et al. 2017. Impacts of open-ocean deep convection in the Weddell Sea on coastal and bottom water temperature. Clim Dyn, 48(9-10): 2967-2981, doi:10.1007/s00382- 016-3244-y.

Ward J M. 2018. Multi-temporal variability within Antarctic coastal polynyas and their relationships to large-scale atmospheric phenomena. PhD Thesis, Carlifornia: University of California, Los Angeles.

Weijer W, Veneziani M, Stössel A, et al. 2017. Local atmospheric response to an open-ocean polynya in a high-resolution climate model. J Clim, 30(5): 1629-1641, doi:10.1175/jcli-d-16-0120.1.

Wendler G, Stearns C, Weidner G, et al. 1997. On the extraordinary katabatic winds of Adélie Land. J Geophys Res: Atmos, 102(D4): 4463-4474, doi:10.1029/96JD03438.

Wenta M A, Cassano J J. 2020. The atmospheric boundary layer and surface conditions during katabatic wind events over the Terra Nova Bay Polynya. Remote Sens, 12(24): 4160, doi:10.3390/rs12244160.

White W B, Peterson R G. 1996. An Antarctic circumpolar wave in surface pressure, wind, temperature and sea-ice extent. Nature, 380(6576): 699-702, doi:10.1038/380699a0.

Whitworth III T, Orsi A H. 2006. Antarctic Bottom Water production and export by tides in the Ross Sea. Geophys Res Lett, 33(12): L12609, doi:10.1029/2006GL026357.

Williams G D, Herraiz-Borreguero L, Roquet F, et al. 2016. The suppression of Antarctic bottom water formation by melting ice shelves in Prydz Bay. Nat Commun, 7: 12577, doi:10.1038/ncomms 12577.

Willmott A J, Holland D M, Morales Maqueda M A. 2007. Chapter 3 Polynya modelling//Smith W O, Barber D G. Polynyas: windows to the world (Volume 74). Amsterdam: Elsevier, 87-125, doi:10.1016/s 0422-9894(06)74003-x.

Yabuki T, Suga T, Hanawa K, et al. 2006. Possible source of the Antarctic bottom water in the Prydz Bay Region. J Oceanogr, 62(5): 649-655, doi:10.1007/s10872-006-0083-1.

Yoon S T, Lee W S, Stevens C, et al. 2020. Variability in high-salinity shelf water production in the Terra Nova Bay Polynya, Antarctica. Ocean Sci, 16(2): 373-388, doi:10.5194/os-16-373-2020.

Yuan X J, Martinson D G. 2000. Antarctic sea ice extent variability and its global connectivity. J Climate, 13(10): 1697-1717, doi:10.1175/1520-0442(2000)013<1697: asieva>2.0.co;2.

Zhang Z R, Uotila P, Stössel A, et al. 2018. Seasonal southern hemisphere multi-variable reflection of the Southern Annular Mode in atmosphere and ocean reanalyses. Clim Dyn, 50(3-4): 1451-1470, doi:10.1007/s 00382-017-3698-6.

Zhang Z R, Vihma T, Stössel A, et al. 2015. The role of wind forcing from operational analyses for the model representation of Antarctic coastal sea ice. Ocean Modelling, 94: 95-111, doi:10.1016/j.ocemod.2015. 07.019.

Zheng F, Li J P, Clark R T, et al. 2013. Simulation and projection of the Southern Hemisphere annular mode in CMIP5 models. J Clim, 26(24): 9860-9879, doi:10.1175/jcli-d-13-00204.1.

Zwally H J, Comiso J C, Gordon A L. 1985. Antarctic offshore leads and polynyas and oceanographic effects//Jacobs S S. Oceanology of the Antarctic continental shelf. Washington, D. C.: American Geophysical Union, 203-226, doi:10.1029/ar043p0203.

Zwally H J, Comiso J C, Parkinson C L, et al. 2002. Variability of Antarctic sea ice 1979–1998. J Geophys Res: Oceans, 107(C5): 9-1-9-19, doi:10.1029/2000JC000733.